Electronic Supplementary Material (ESI) for Journal of Materials Chemistry C.

Electronic Supplementary Information

For

Disentangling the Complex Photodynamics of Mixed-Linker Zr-MOFs - Efficient Energy and Charge Transfer Processes

Mario Gutiérrez[#a], Maria Rosaria Di Nunzio[#a], Elena Caballero-Mancebo[a], Félix Sánchez, Boiko Cohen[*a], and Abderrazzak Douhal[*a]

[a.] Departamento de Química Física, Facultad de Ciencias Ambientales y Bioquímica, INAMOL, Universidad de Castilla-La Mancha, Avenida Carlos III, S.N., 45071 Toledo, Spain.

[b.] Instituto de Química Orgánica, CSIC, Juan de la Cierva, 3, 28006 Madrid, Spain.

*corresponding authors: Boyko.koen@uclm.es; abderrazzak.douhal@uclm.es

# Equal Contributions.

Table of Contents

Characterization

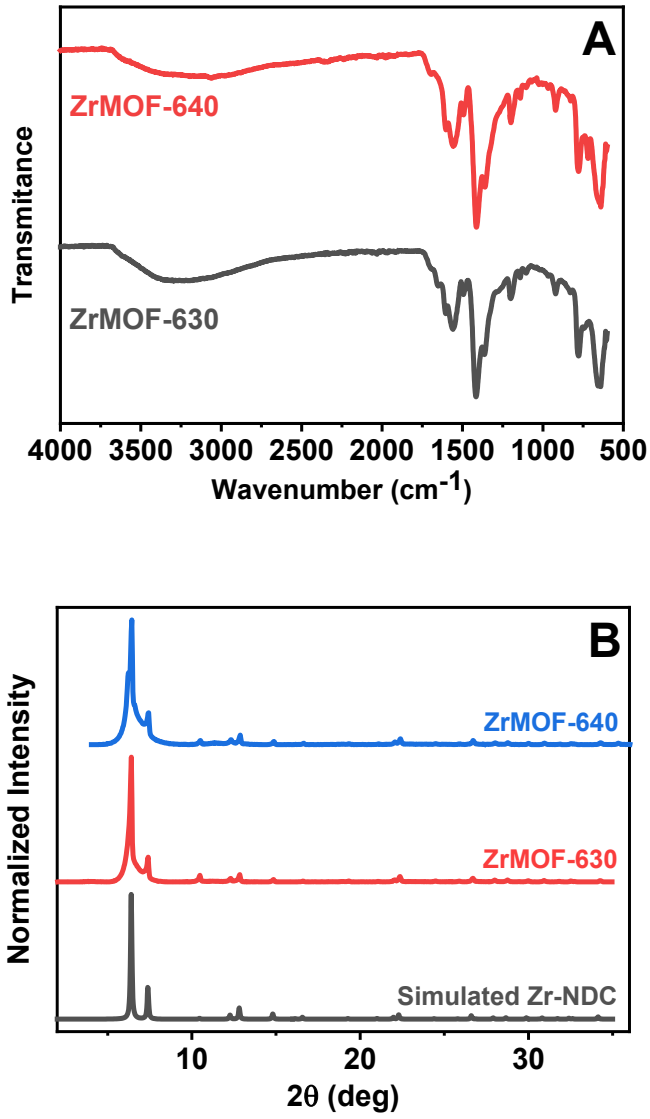

Figure S1. (A) FTIR spectra of ZrMOF-630 (dark grey line) and ZrMOF-640 (red line). (B) Powder X-ray diffraction (PXRD) patterns of ZrMOF-630 and ZrMOF-640 and their comparison with the simulated pattern of Zr-NDC MOF.

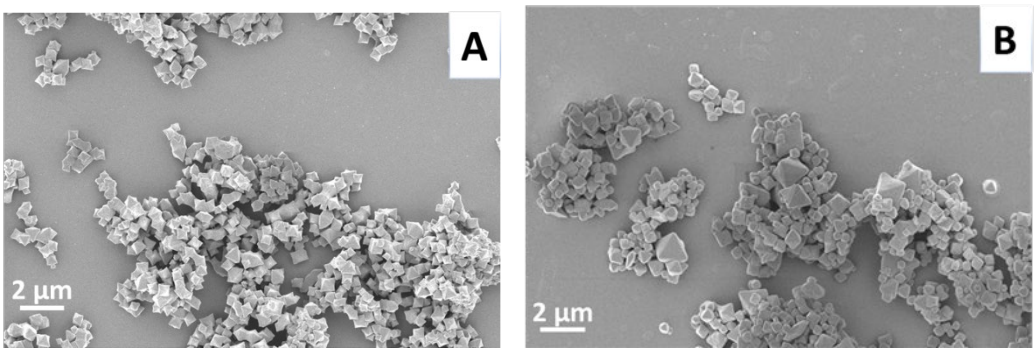

Figure S2. SEM images of (A) ZrMOF-630 and (B) ZrMOF-640.

UV-Vis Steady-State Experiments

Solvent Suspensions

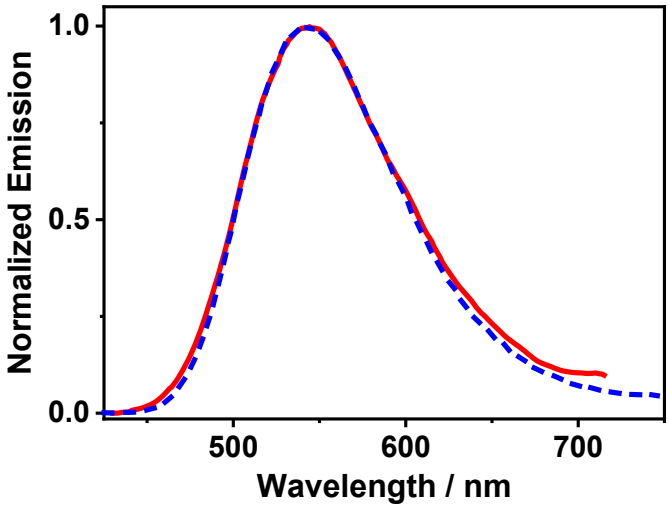

Figure S3. Normalized (to the maximum of intensity) emission (λ_{exc} = 400 nm) spectra of ZrMOF-630 (red solid lines) and ZrMOF-640 (blue dashed lines).

System	Solvent	λ_{exc}/nm	PLQY ± 0.01
ZrMOF-630	Dichloromethane	355	0.04
	Diethyl ether		0.04
	Methanol		0.03
	Dichloromethane	430	0.02
	Diethyl ether		0.03
	Methanol		0.02
ZrMOF-640	Dichloromethane	355	0.05
		430	0.03

Table S1. Photoluminescence quantum yields (PLQYs) of ZrMOF-630 and ZrMOF-6340 in different solvent suspensions upon excitation at 350 and 400 nm.

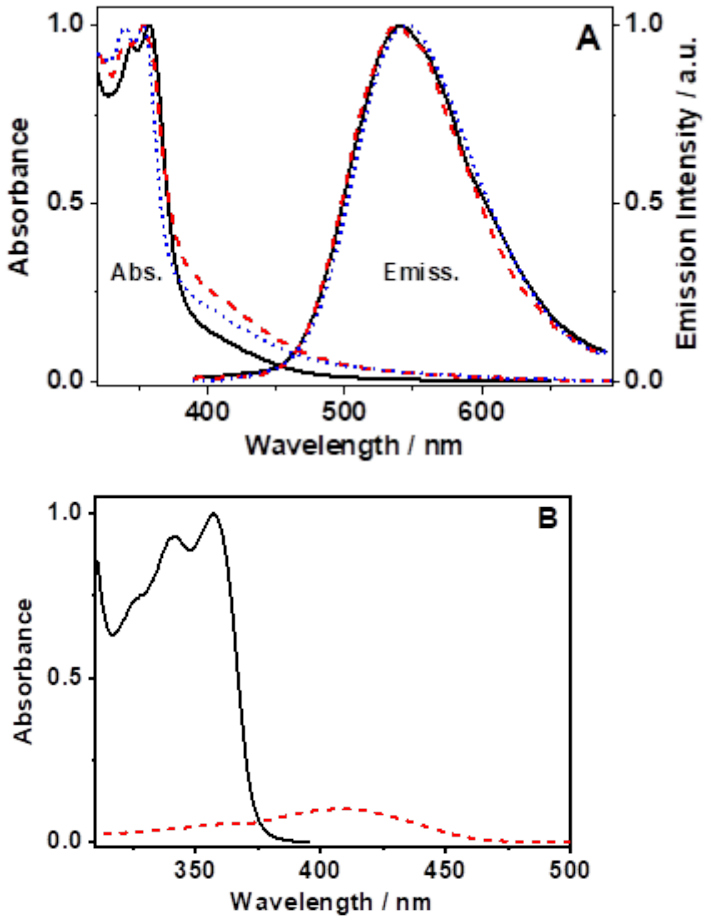

Figure S4. (A) Normalized (to the maximum of intensity) UV-visible absorption and emission spectra of ZrMOF-630 in dichloromethane (DCM, black solid lines), diethyl ether (DE, red dashed lines), and methanol (MeOH, blue dotted lines) suspensions. The emission spectra were recorded upon excitation at 355 nm. (B) Absorption spectrum of NDC (solid line) and NACDC (dashed line) linkers in DCM solutions and considering their relative proportion (90% of NDC and 10% of NACDC) in ZrMOF-630 and ZrMOF-640.

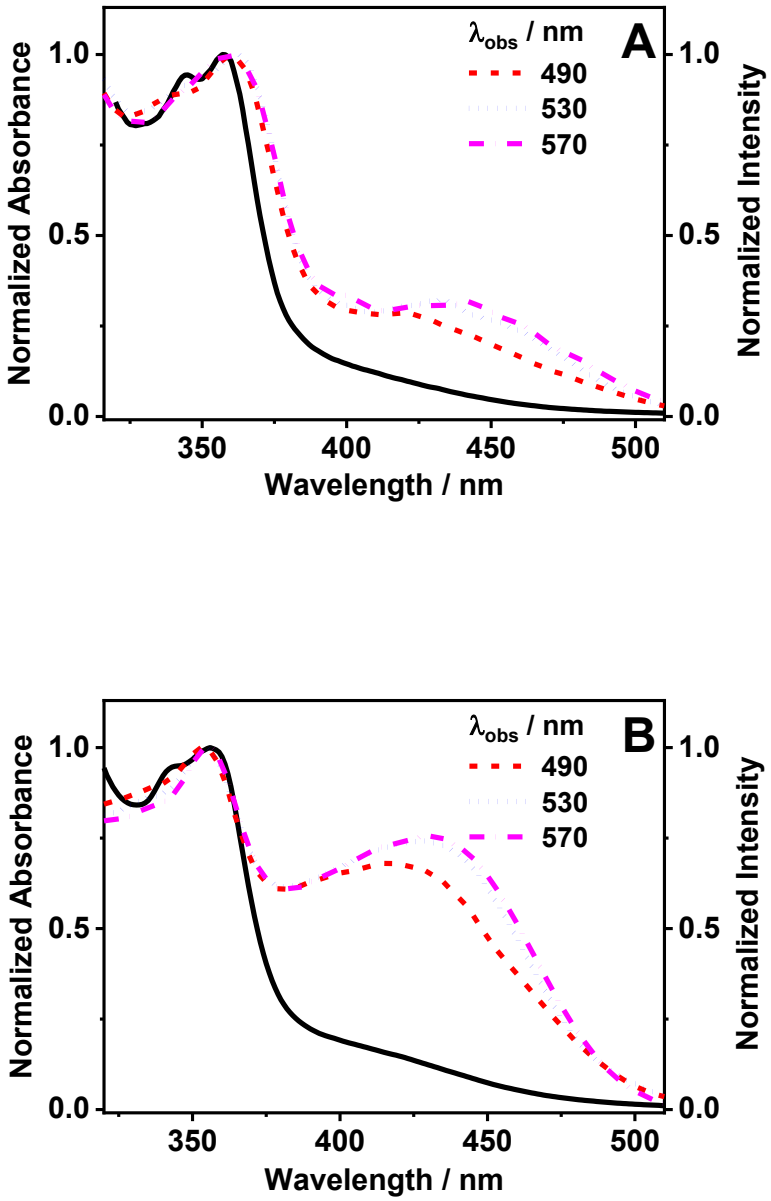

Figure S5. Normalized (to the maximum of intensity) UV-visible absorption (black, solid line) and excitation (colored, no-solid lines) spectra of (A) ZrMOF-630 and (B) ZrMOF-640 in DCM suspensions. The observation wavelengths are indicated in the Inset.

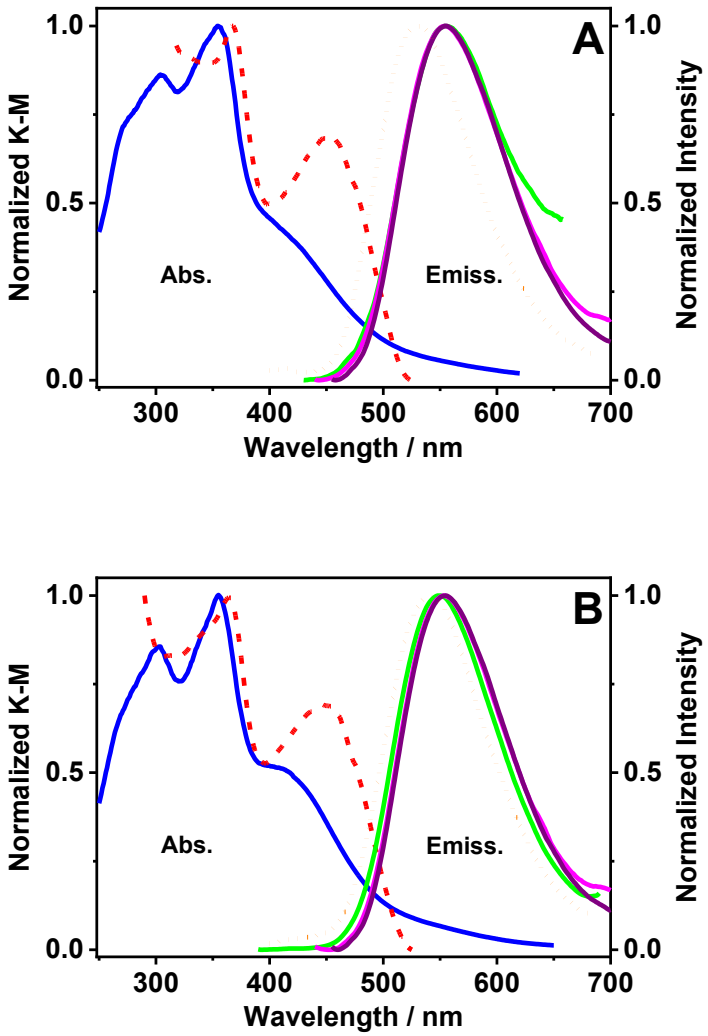

Figure S6. Normalized (to the maximum of intensity) UV-visible reflectance (converted to K-M, solid lines), excitation (λ_{em} = 550 nm; dashed lines), and emission (λ_{exc} = 355, 390, and 433 nm; solid lines) spectra of (A) ZrMOF-630 and (B) ZrMOF-640 in the solid-state. The emission (λ_{exc} = 355 nm; dotted lines) spectra of ZrMOF-630 and ZrMOF-640 in DCM suspensions are showed for comparison.

Picosecond-Time-Resolved Experiments

DCM Suspensions

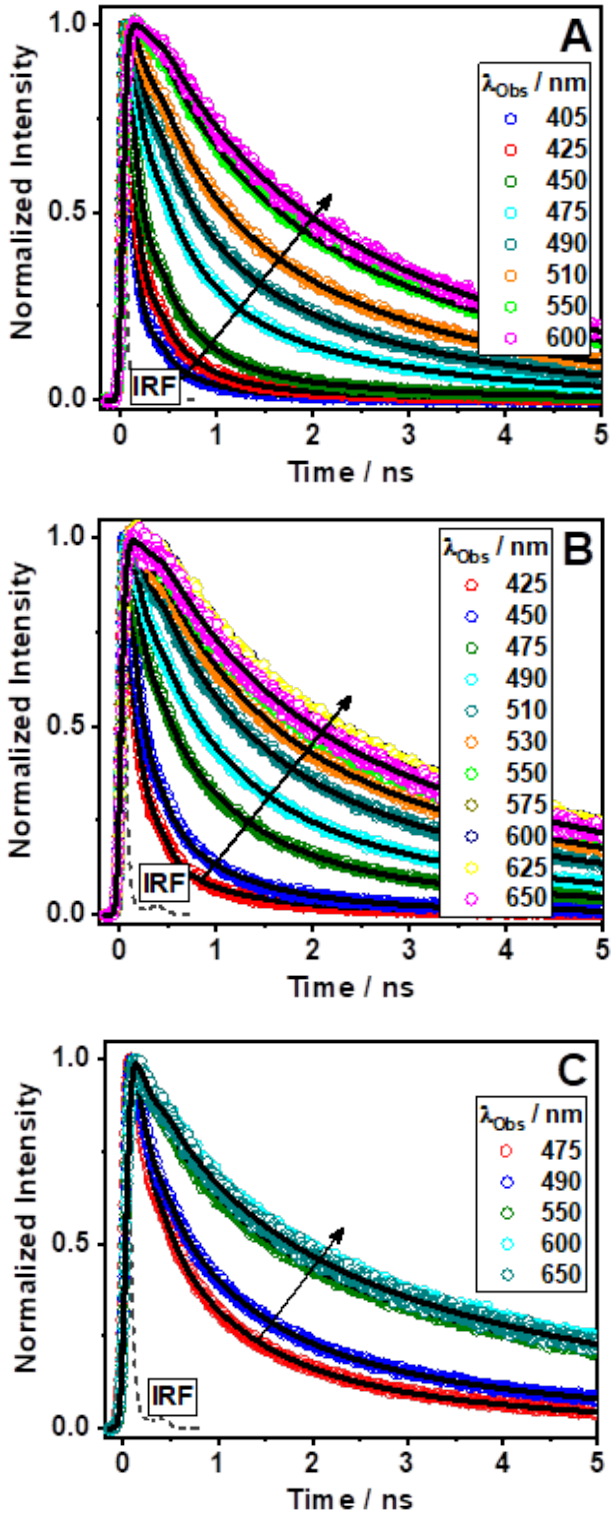

Figure S7. Normalized (to the maximum of intensity) magic-angle ps-emission decays of ZrMOF-630 in DCM suspensions upon excitation at (A) 340, (B) 371, and (C) 433 nm and observation at the indicated wavelengths. The solid lines are from the best fit of the experimental data.

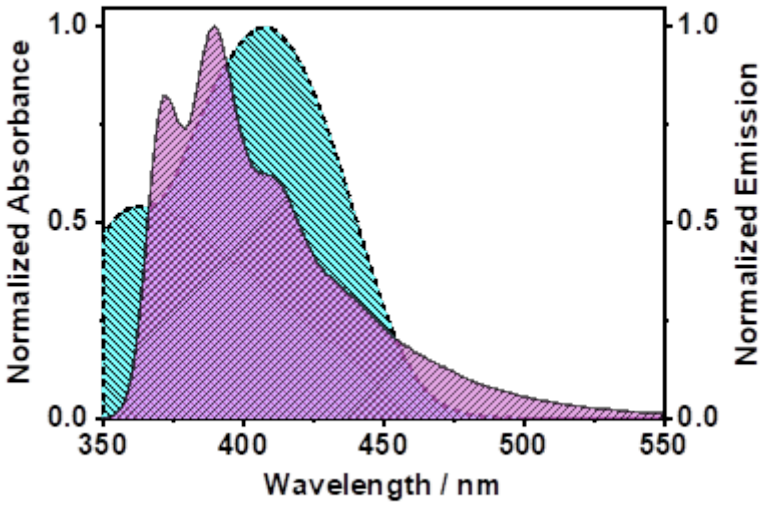

Figure S8. Normalized emission (solid line) and absorption (dashed line) spectra of Zr-NDC and Me_2NACDC linker, respectively, in DCM.

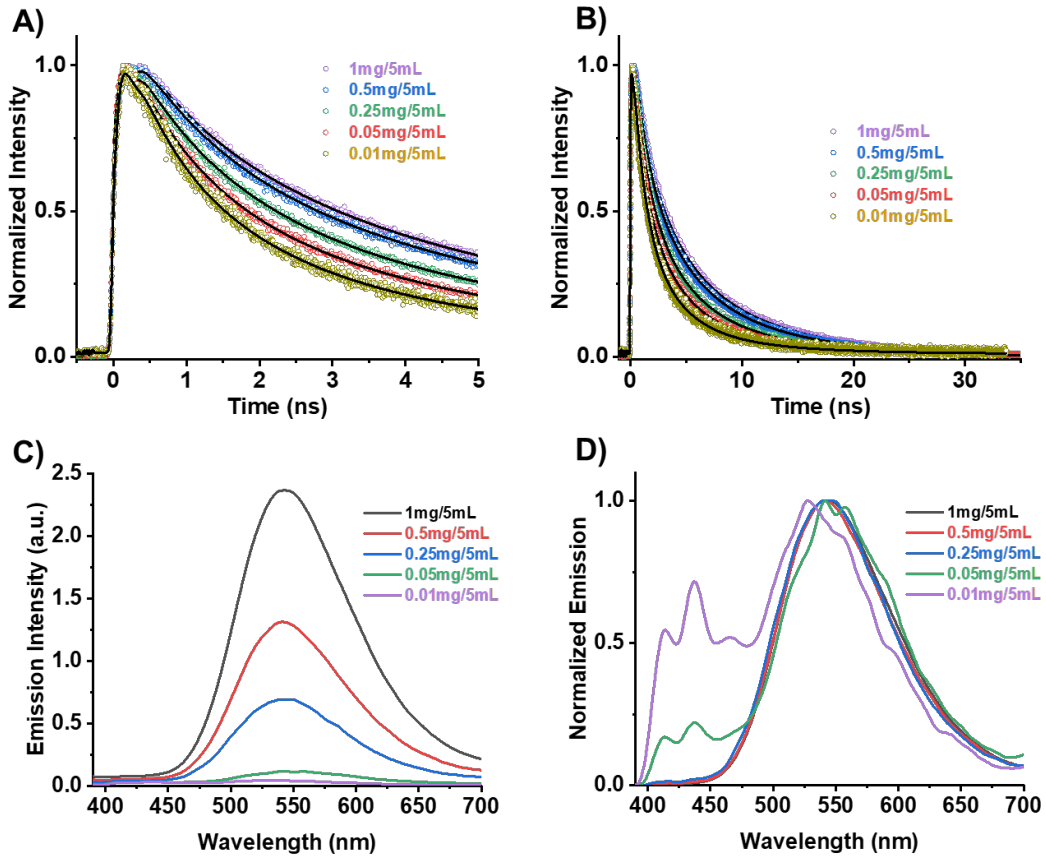

Figure S9. Normalized (to the maximum of intensity) magic-angle ps-emission decays of different concentrated suspensions of ZrMOF-630 in DCM upon excitation at 371 nm and observation at 550 nm, represented in a short (A) and long (B) temporal windows. The solid lines are from the best fit of the experimental data. (C, D) are the (C) emission and (D) normalized to the maximum emission spectra of the different suspensions of ZrMOF-630 in DCM. The excitation wavelength was 371 nm.

Sample	λobs /nm	τ1/ps ± 15	a1	c1	τ2/ps ± 50	a2	c2	τ3/ns ± 0.2	a3	c3	τ4/ns ± 0.3	a4	c4
MOF630 1 mg/ 5ml	**550**	**150**	-100	-100	**990**	25	5	**3.5**	43	32	**9.5**	32	63
MOF630 0.5 mg/ 5ml	**550**	**110**	-100	-100	**980**	30	7	**3.6**	43	35	**9.4**	27	58
MOF630 0.25 mg/ 5ml	**550**	**30**	-100	-100	**990**	36	10	**3.3**	43	39	**8.7**	21	51
MOF630 0.05 mg/ 5ml	**550**	**20**	-100	-100	**860**	39	11	**2.9**	42	41	**8.2**	19	48
MOF630 0.01 mg/ 5ml	**550**	**<10**	-100	-100	**950**	50	19	**2.9**	39	46	**8.5**	11	34

Table S2. Values of time constants (τ_i) normalized (to 100) pre-exponential factors (a_i), and contributions (c_i) obtained from the multi-exponential fit of the emission decays of different concentrated suspensions of ZrMOF-630 in DCM, as indicated in the Table. The excitation wavelength was 371 nm.

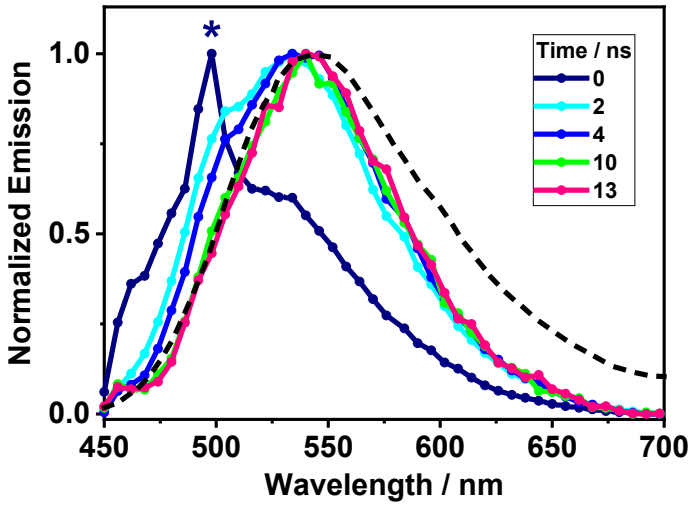

Figure S10. Normalized (to the maximum of intensity) ps-time-resolved emission spectra (TRES) of ZrMOF-630 in DCM suspensions upon excitation at 433 nm at different delays as indicated in the inset. The dashed spectrum corresponds to the steady-state emission upon excitation at 400 nm. The symbol (*) indicates that in this spectral region and at the shortest time delays the total signal is a sum of sample emission and Raman scattering from DCM, having the latter its maximum at ~500 nm.

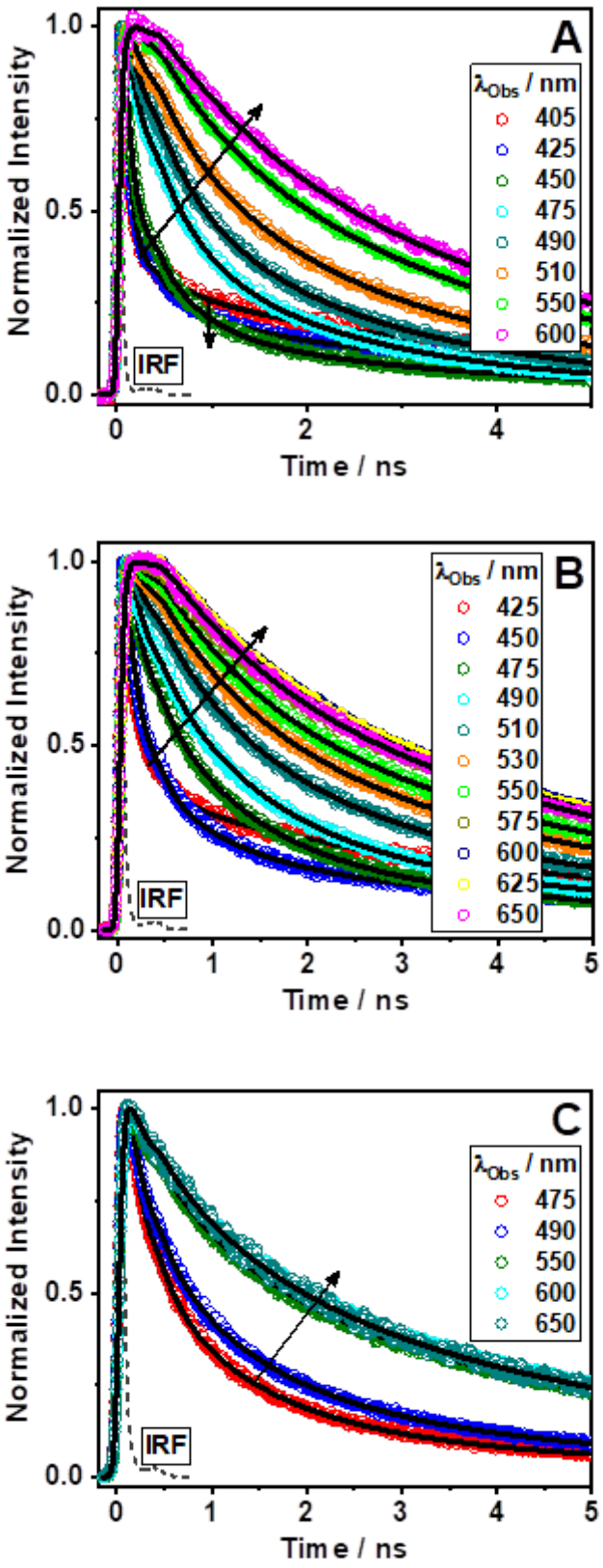

Figure S11. Normalized (to the maximum of intensity) magic-angle ps-emission decays of ZrMOF-640 in DCM suspensions upon excitation at (A) 340, (B) 371, and (C) 433 nm and observation at the indicated wavelengths. The solid lines are from the best fit of the experimental data.

Solid-State

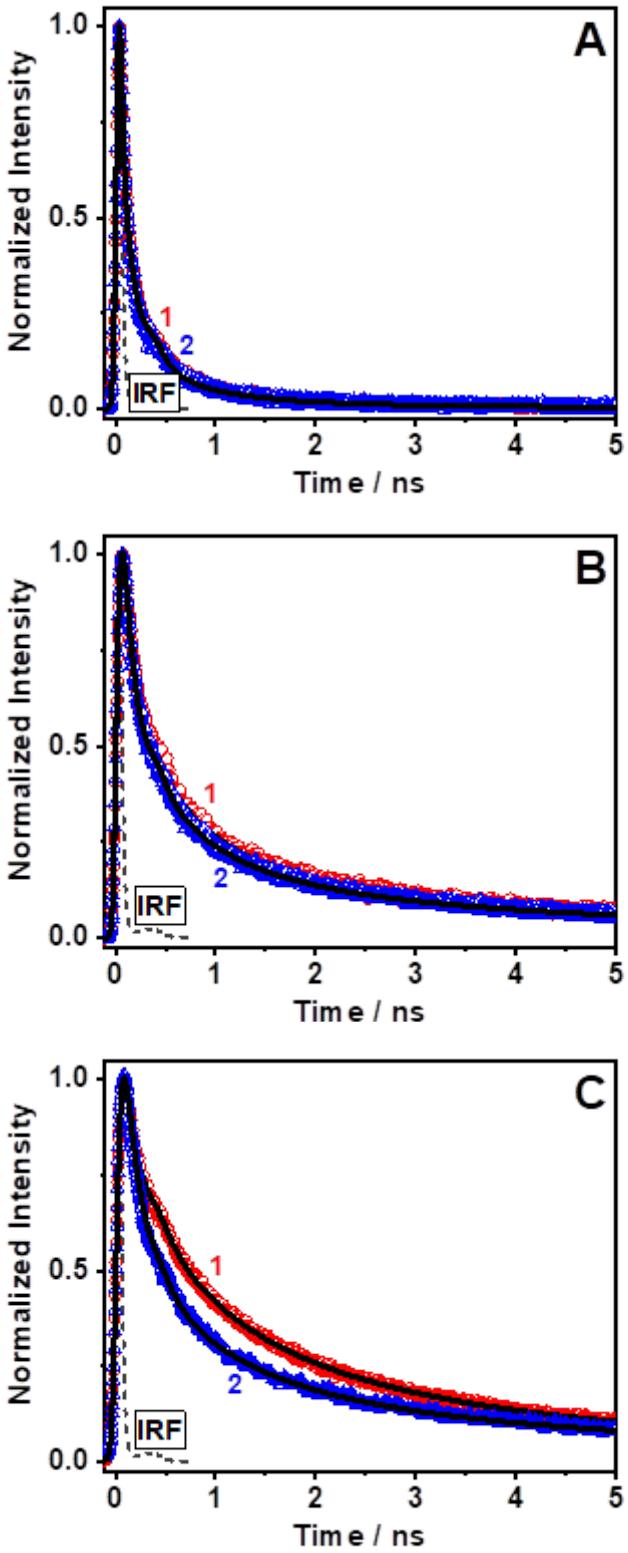

Figure S12. Normalized (to the maximum of intensity) magic-angle ps-emission decays of (1) ZrMOF-630 (red circles) and (2) ZrMOF-640 (blue triangles) in the solid-state upon excitation at (A,B) 371 and (C) 433 nm and observation at (A) 450 and (B,C) 650 nm. The solid lines are from the best fit of the experimental data.

Sample	λ_{obs} /nm	τ_1/ps ± 15	a_1	c_1	τ_2/ps ± 50	a_2	c_2	τ_3/ns ± 0.2	a_3	c_3	τ_4/ns ± 0.3	a_4	c_4
630 λ_{exc} = 371 nm	450	110	80	29	600	17	33	2.5	2	15	8.6	1	23
	500		51	7		32	23		14	42		3	28
	550		29	2		34	11		26	35		11	52
	600		35	2		30	10		23	33		12	55
	650		57	7		27	17		11	29		5	47
640 λ_{exc} = 371 nm	450	130	85	37	720	13	32	2.9	1	14	9.0	1	17
	500		57	9		29	27		12	42		2	22
	550		55	6		24	14		15	35		6	45
	600		47	4		26	12		18	32		9	52
	650		68	10		20	18		8	27		4	45
630 λ_{exc} = 433 nm	500	170	50	8	890	32	26	3.0	15	43	8.7	3	23
	550		45	5		29	17		19	39		7	39
	600		45	5		27	14		20	37		8	44
	650		47	5		27	16		19	40		7	39
640 λ_{exc} = 433 nm	500	150	48	7	810	33	26	2.7	16	42	8.5	3	25
	550		38	3		30	15		24	39		8	43
	600		43	4		28	14		20	33		9	49
	650		41	6		30	16		20	34		9	44

Table S3. Values of time constants (τ_i), normalized (to 100) pre-exponential factors (a_i), and contributions (c_i) obtained from the multi-exponential fit of the emission decays of ZrMOF-630 and ZrMOF-640 in the solid-state upon excitation at 371 and 433 nm and observation as indicated in the Table.

Single Crystal Fluorescence Microscopy Results

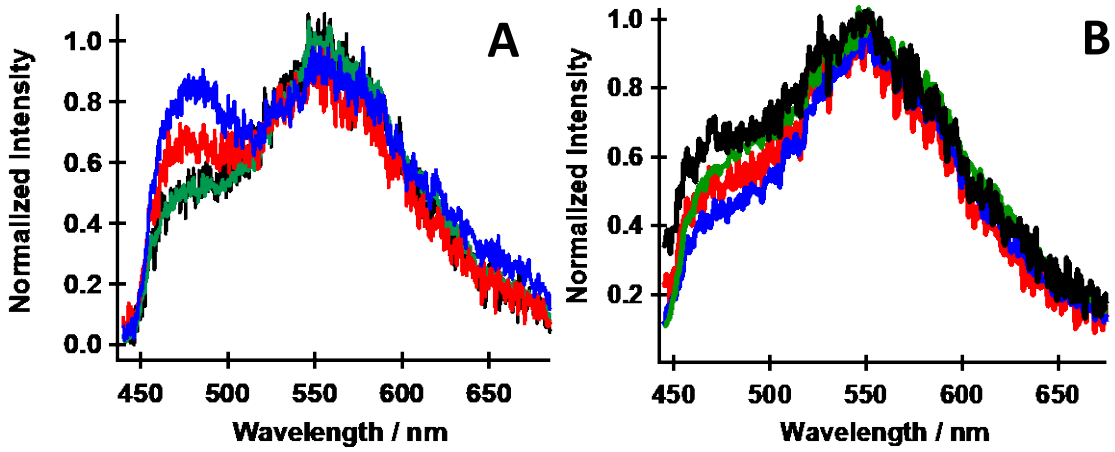

Figure S13. Representative emission spectra of 4 isolated single A) ZrMOF-630 and B) ZrMOF-640 crystals monitored with confocal microscopy. The excitation wavelength was 390 nm.T he spectra were smoothed by 7 point binomial method for clarity of presentation.

Femtosecond-Transient Absorption Results

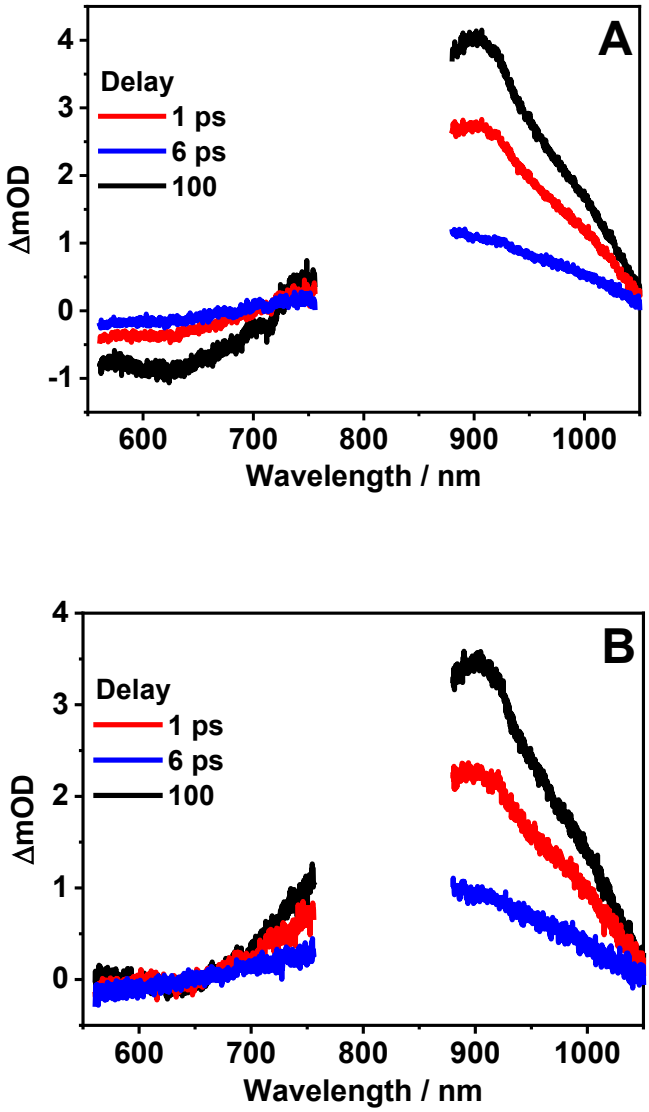

Figure S14. Time evolution of the transient absorption spectrum (TAS) of A) MOF630 and B) MOF640 in a DCM suspension in terms of the change in the optical density (DOD) upon excitation at 360 nm at the indicated delay times.

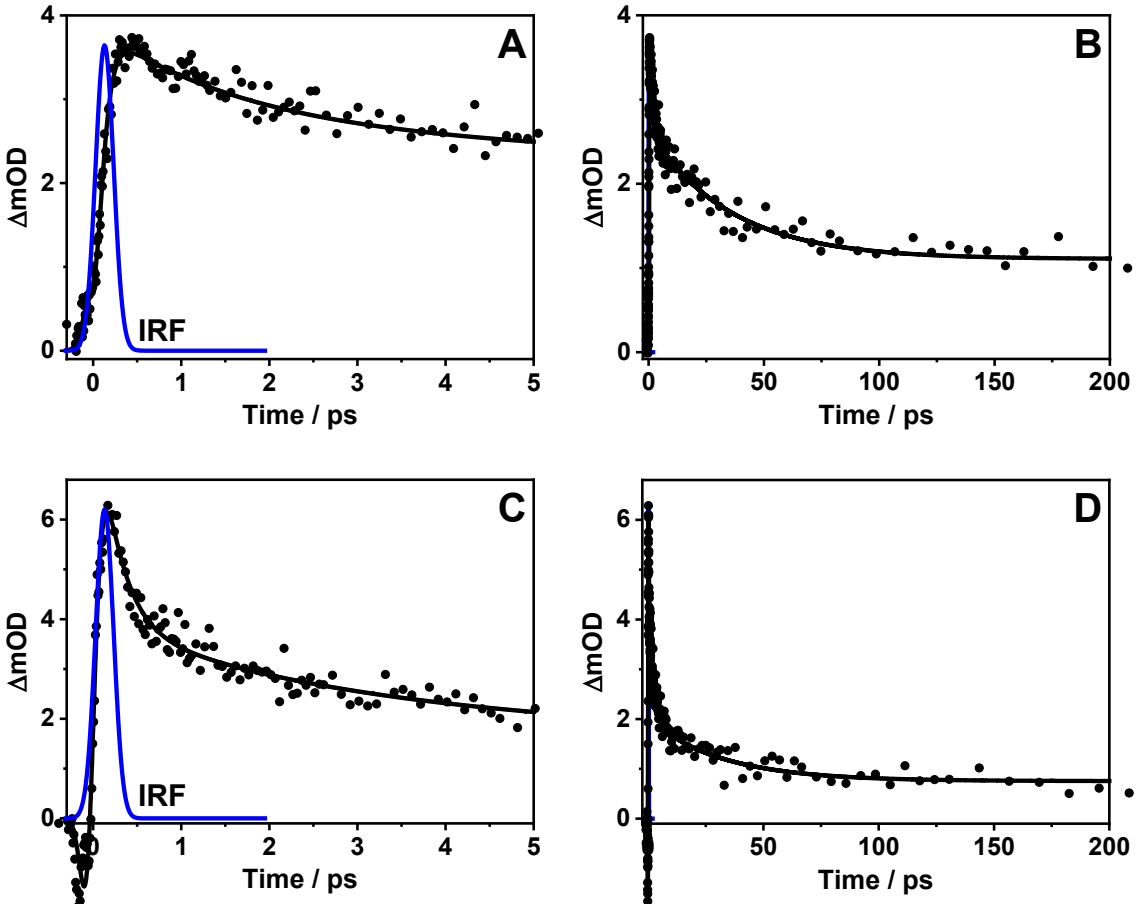

Figure S15. Femtosecond transient absorption decays at 920 nm in terms of changes in the optical density (ΔOD) of MOF640 in DCM following excitation at 360 nm: A) short and B) long time windows; and following excitation at 420 nm: C) short and D) long time windows. The solid lines are from the best multiexponential fits, and the IRF is the instrumental response function. Note that the initial decay of the signal, following excitation at 420 nm (C and D), is affected by the ultrafast solvent response at this excitation wavelength.

Microsecond-Transient Absorption Experiments

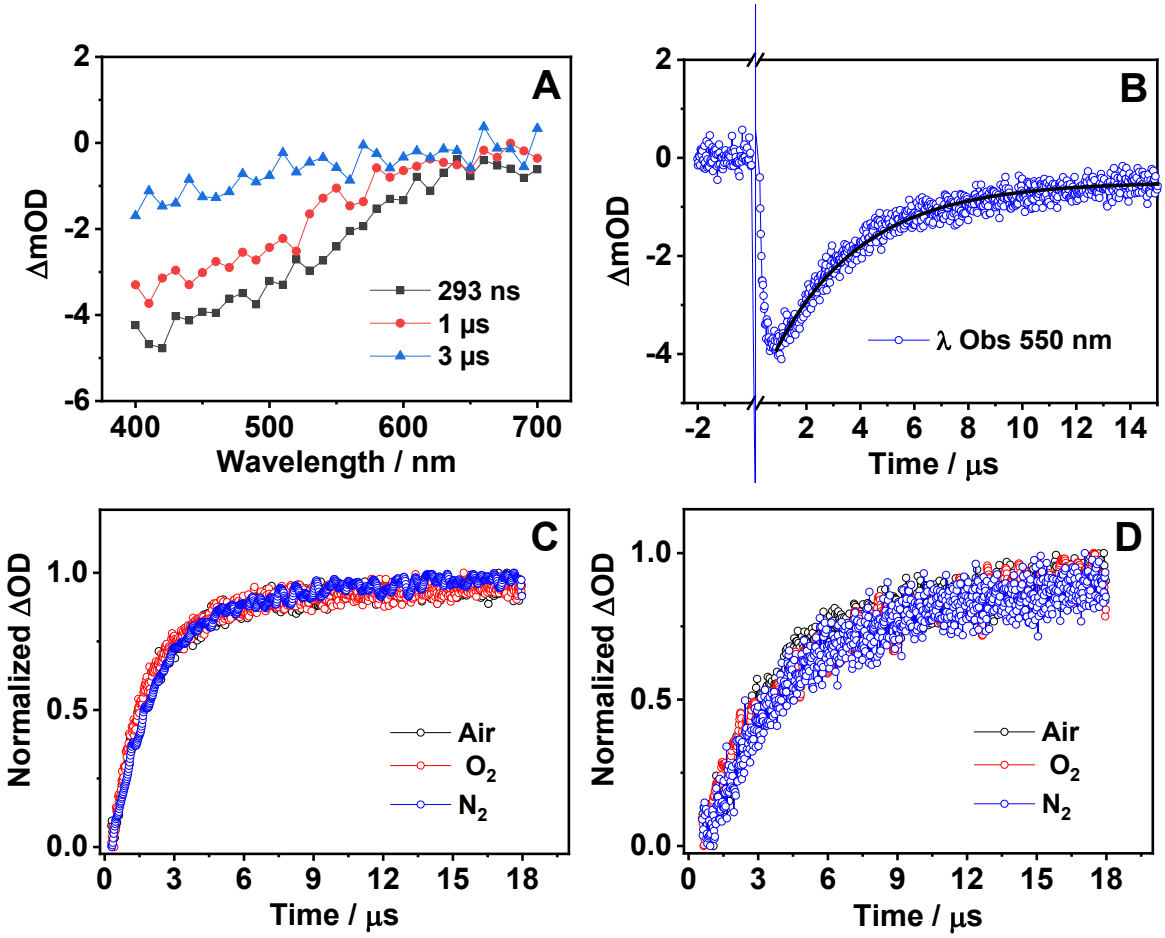

Figure S16. (A) Time evolution of the TAS of excited ZrMOF-630 in DCM suspensions. The excitation wavelength and the delay time of each spectrum are indicated in the Inset. (B,C) Transient decays of (B) ZrMOF-630 and (C) ZrMOF-640 in DCM suspensions exciting at 355 nm and observing at 550 nm under different atmospheric conditions: air (black), oxygen (red), and nitrogen (blue). The time of gas bubbling into the cuvette was five minutes for all the cases.